Available online at www.sciencedirect.com

SCIENCE DIRECT

Experimental Cell Research 306 (2005) 47–55

Experimental Cell Research

www.elsevier.com/locate/yexcr

Loss of the *Dictyostelium* RasC protein alters vegetative cell size, motility and endocytosis

Chinten James Lim*, Karl A. Zawadzki[1], Meenal Khosla, David M. Secko, George B. Spiegelman, Gerald Weeks

Department of Microbiology and Immunology, University of British Columbia, Vancouver, British Columbia, Canada V6T1Z3

Received 19 October 2004, revised version received 3 February 2005
Available online 11 March 2005

Abstract

In addition to its previously established roles in cAMP relay and cAMP chemotaxis, loss of signal transduction through the RasC protein was found to impact a number of vegetative cell functions. Vegetative *rasC*$^{-}$ cells exhibited reduced random motility, were less polarized and had altered F-actin distribution. Cells lacking RasC also contained more protein and were larger in size than wild type cells. These increases were associated with increased liquid phase endocytosis. Despite the increase in cell size, cytokinesis was relatively normal and there was no change in the rate of cell division. *rasC*$^{-}$ cells also chemotaxed poorly to folate and exhibited reduced F-actin accumulation, reduced ERK2 phosphorylation and reduced Akt/PKB phosphorylation in response to folate, indicating that RasC was also involved in transducing chemotactic signals in vegetative cells.
© 2005 Elsevier Inc. All rights reserved.

Keywords: Cell size; Cytoskeleton; Endocytosis; Folate; Motility; Ras; Akt/PKB; ERK2

Introduction

The Ras subfamily proteins are monomeric GTPases that function as molecular switches by cycling between the active GTP-bound or inactive GDP-bound state [1]. In the active state, inputs through Ras proteins are linked to multiple cellular signaling pathways that include mitogen activated protein kinase (MAPK) cascades, phosphotidylinositide 3-kinase (PI3K) regulated pathways and RalGDS dependent activation of Ral [2]. These Ras-mediated responses to membrane receptor stimuli impinge on a wide range of cellular processes, including proliferation, cytoskeletal functions and differentiation.

The discovery of a large number of Ras subfamily homologues in mammals and in the model organisms *Drosophila melanogaster*, *Caenorhabditis elegans* and *Dictyostelium discoideum* [3,4] has raised important questions regarding the specific functions of individual Ras proteins. As one approach to understanding Ras function in a cellular context, we have undertaken analysis of *Dictyostelium* strains that are genetically disrupted in the *ras* gene of interest.

Six *Dictyostelium* Ras subfamily proteins with at least 50% amino acid identity to the mammalian H, N and K-Ras proteins have been described [5,6]. Four of the *Dictyostelium ras* genes, *rasC*, *rasS*, *rasG* and *rasD*, have been disrupted and each of the resulting strains has a distinct phenotype, suggesting that each encoded product performs a distinct function [7–9]. Attempts at generating stable disruptants of the *rap1* and *rasB* genes have been unsuccessful and the available evidence is consistent with the idea that both these genes are essential for growth [10,11].

* Corresponding author. Present address: Division of Rheumatology, Department of Medicine, University of California San Diego, La Jolla, CA 92093-0726, USA. Fax: +1 858 8226458.
E-mail address: cjlim@ucsd.edu (C.J. Lim).
[1] Present address: Department of Molecular Biology, Princeton University, Princeton, NJ 08544, USA.

0014-4827/$ - see front matter © 2005 Elsevier Inc. All rights reserved.
doi:10.1016/j.yexcr.2005.02.002

In a previous report, we showed that the targeted disruption of the *Dictyostelium rasC* gene results in cells that fail to aggregate, indicating that RasC plays an essential role during the aggregation phase of starvation-induced multicellular development [12]. During early development, RasC appears to transmit signals downstream of cAMP receptor stimulation that are required for the optimal functioning of both cAMP relay and chemotaxis to cAMP. The severity of the chemotaxis defect depends upon the experimental conditions employed. Thus, when starved in buffer, *rasC*$^-$ cells exhibit only very slow chemotaxis towards cAMP, but following exposure to periodic pulses of cAMP, the cells are capable of rapid and efficient chemotaxis in a spatial cAMP gradient [12]. More detailed analysis revealed that starved, cAMP-pulsed *rasC*$^-$ cells exhibit abnormal pseudopod dynamics when subjected to a temporal cAMP wave [13], indicating that RasC is required for wild type chemotactic behavior. Other experiments to examine the integrity of signal transduction pathways indicated that there is sub-optimal activation of both Akt/PKB and adenylyl cyclase in response to cAMP in *rasC*$^-$ cells.

During the course of these studies, it became apparent that vegetative *rasC*$^-$ cells also exhibited abnormalities, indicating that RasC also had functions in growing cells. In this report, we describe a detailed examination of the properties of vegetative *rasC*$^-$ cells.

Materials and methods

Cell growth and maintenance

D. discoideum cells were grown axenically in HL5 medium supplemented with 10 μg/ml streptomycin (Sigma) at 22°C in suspension in flasks shaken at 150 rpm [14]. The *rasC*$^-$ and parental AX2 strain have been described previously [12]. The AX2/RasC overexpression strain was generated by transforming AX2 with the *rasC*::*rasC* expression vector. For growth curve assays, cells were seeded at an initial density of 10^5 cells/ml in flasks of HL5. Cell densities at various time points were determined by counting using a hemocytometer.

Cell migration

To assay the random motility of vegetative amoebae, cells were seeded at low density (~2×10^4 cells/cm^2) on Nunc plastic dishes in HL5 media and allowed to adhere for 1 h. The low cell density facilitates tracking of individual cell movements within the field of view over the course of the assay. A time-lapse movie was compiled by capturing an image of the cells every minute for 1/2 h using Scion Image and a CCD camera coupled to an Olympus CX inverted microscope viewed through a 10× objective. The centroid position for each cell in all 30 image frames was marked, and the centroids connected with a line to reveal a continuous trace for a single amoeba over 30 min. The point of origin for all the individual amoeba tracks was positioned to the centre of a field of view using Adobe Photoshop to superimpose the images. The result is an image of 30 amoeba tracks that appear to radiate outwards from the centre.

For the transwell chemotaxis assay, 10^5 cells in HL5 were added to the top chamber of a Costar 24-well transwell plate (Cat 3421) with 5.0 μm pores. 1 μM folate in HL5 was then applied to the bottom chamber. The number of cells that migrated to the underside of each transwell membrane was visually scored after 1 h by analyzing randomly selected fields of view. Folate micropipet assays were adapted from a previously described protocol [15]. Cells were cultivated in HL5 media on Nunc tissue culture dishes to a density of ~4×10^5 cells/cm^2. The cells were then rinsed once and submerged in 20% HL5. At $t = 0$, a micropipet (Eppendorf Femtotips) filled with 25 mM folate was positioned in the field of view and cell movements monitored by time-lapse microscopy.

F-actin assays

For visualization of F-actin distribution in situ, cells grown and maintained in HL5 media in Nunc tissue culture dishes were reseeded onto glass coverslips and allowed to adhere for 3 h. The cells were then fixed and permeabilized with 1% glutaraldehyde, 0.1% Triton X-100 in PBS for 10 min. Fixed cells were rinsed three times in phosphate buffered saline (PBS) and autofluorescence quenched with 1 mg/ml NaBH for 10 min. Following three further rinses in PBS, the cells were stained with 0.1 μg/ml fluorescein isothiocyanate (FITC) phalloidin conjugate (Sigma) for 1 h, rinsed in PBS and the coverslips air-dried and mounted onto slides with or without the addition of Prolong antifade (Molecular Probes). Epi-fluorescent images were taken on a Zeiss Axiovert microscope.

For in vitro determination of F-actin levels, suspension grown cells were washed twice, resuspended at 5–7 × 10^6 cells/ml in KK2 (20 mM potassium phosphate, pH 6.1) and shaken at 180 rpm for 30 min. The cells were rewashed twice and resuspended at 4×10^7 cells/ml in KK2. Before and after addition of folate to a final concentration of 50 μM, 100 μl aliquots were removed at the indicated time points and immediately mixed with 1.3 ml fix/stain buffer (2× GB containing 3.7% formaldehyde, 0.1% Triton X-100, 0.5 μM tetramethylrhodamine B isothiocyanate (TRITC)-phalloidin (Sigma); 2× GB is 20 mM PIPES pH 6.8, 20 mM potassium phosphate pH 6.8, 5 mM EGTA, 2 mM $MgSO_4$) and the mixture incubated for 1 h. The cells were then pelleted by centrifugation at 13,000 × *g* for 10 min, and the pellet resuspended in 1.0 ml 0.1% saponin (Sigma) in 2× GB for 1 h. Following centrifugation, the cell pellet was extracted with 1.0 ml methanol overnight at 4°C. After centrifuga-

tion, the fluorescence in the methanol extract was measured in a SpectraMax Gemini XS microplate fluorometer (Molecular Devices) with λ^{Ex} = 525 nm and λ^{Em} = 564 nm. 100 μl aliquots of the cell suspension were also harvested and lysed in 0.5% SDS for protein determination using the DC protein assay (BioRad).

ERK2 and Akt/PKB phosphorylation assays

Suspension grown cells were prepared and stimulated with 50 μM folate exactly as described above for F-actin accumulation, except that 100 μl cell aliquots were removed at the indicated time points and immediately lysed with 20 μl 6× Laemmli gel loading buffer [16] supplemented with 100 mM NaF, 1.2 mM Na_3VO_4, 12 mM EDTA and protease inhibitors (Roche Complete). 10 μg protein samples were fractionated by SDS-PAGE, blotted onto nitrocellulose and probed with the phospho-MAPK antibody and phospho-threonine antibody (Cell Signaling Tech). Equal sample loading was verified by staining a duplicate gel with Coomassie Brilliant Blue. To account for possible variations between multiple blots, standard cell extracts were included in each blot and the ECL autoradiogram signals verified by densitometric analysis (GeneQuant, Molecular Dynamics).

Fluid phase endocytosis assay

6×10^7 cells in logarithmic growth phase were pelleted and resuspended in 15 ml of HL5 media. They were shaken at 160 rpm for 30 min at 22°C, then FITC-dextran (M_r = 70 kDa; Sigma) in 50 mM Na_2HPO_4 was added to a final concentration of 2 mg/ml (t = 0 min). At the indicated time points, 1.0 ml aliquots of the cell suspension was mixed with 9.0 ml ice-cold KK2 and pelleted by centrifugation. The cells were then washed once with 5.0 ml ice-cold KK2 containing 40 μg/ml trypan blue to quench external fluorescence, and once with ice-cold KK2. The final cell pellet was lysed in 0.2% Triton X-100 in 50 mM Na_2HPO_4. The incorporated fluorescence in the lysate was measured using a microplate fluorometer (SpectraMax Gemini XS, Molecular Devices) set at λ^{Ex} = 470 nm and λ^{Em} = 520 nm.

Cell volume and protein determinations

2.4×10^8 logarithmic growth-phase cells were centrifuged for 5 min at 3300 g in a Pyrex No. 8082 tapered graduated test tube and the volume occupied by the resulting pellet determined. For protein determinations, triplicate samples were taken from exponentially growing, shake suspension cultures, centrifuged for 5 min at 3300 × g and the cell pellet resuspended in 1% SDS. Protein was determined using the DC protein assay (Bio-Rad) and values are expressed as the amount of protein (mg) contained in 10^8 cells.

Nuclear staining

Cells grown to logarithmic phase ($2–4 \times 10^6$ cells/ml) in shake suspension were seeded and allowed to adhere on glass coverslips for 20 min. The media was removed and the cells were fixed with methanol for 10 min at −20°C. Fixed cells were washed three times with 1× PBS, and the nuclei stained with 1 μM 4,6-diamidino-2-phenylindole (DAPI, Sigma) in 1× PBS for 10 min. Stained cells were washed three times with 1× PBS, air-dried and mounted on glass slides with 50% glycerol. Epifluorescence and phase contrast images of random fields of view were captured through an Olympus IX-70 inverted microscope using a DAGE CCD100 camera, a Scion VG5 framegrabber and Scion Image 4.0.

Cell area

Cells grown to logarithmic phase ($2–4 \times 10^6$ cells/ml) in shake suspension were placed on glass coverslips and viewed within 10 min. Phase contrast images of the cells were taken and analyzed with ImageJ software (NIH). Due to the irregular nature of their shapes, the area occupied by the cell was measured instead of the cell diameter.

Results

Folate chemotaxis

In the absence of pre-exposure to periodic pulses of cAMP, starving *rasC*$^-$ cells chemotax slowly along a spatial gradient of cAMP [12], suggesting that RasC is involved in the response to this chemoattractant. To investigate if RasC is also involved in chemotaxis to folate, a known chemoattractant for vegetative *Dictyostelium* cells [17], we determined the movement of vegetative wild type AX2 and *rasC*$^-$ cells in a folate spatial gradient, formed by diffusion from a folate-filled micropipet. After 50 min, numerous AX2 cells had moved towards the micropipet (Fig. 1, top panels), whereas a similar movement of *rasC*$^-$ cells was not detected until after 100 min (Fig. 1, bottom panels), suggesting an involvement of RasC in the response to folate. However, transwell chamber assays revealed that *rasC*$^-$ cells traversed the membrane more slowly than AX2 cells, both in the presence and absence of a folate gradient (data not shown). Thus, loss of RasC might adversely affect vegetative cell motility in general, rather than specifically affecting signals that determine directional cell movement to folate.

General motility

To investigate whether the loss of RasC altered cellular motility in general, we analyzed the movement of individual vegetative AX2 and *rasC*$^-$ cells in the absence of a chemoattractant. Cells were allowed to adhere to

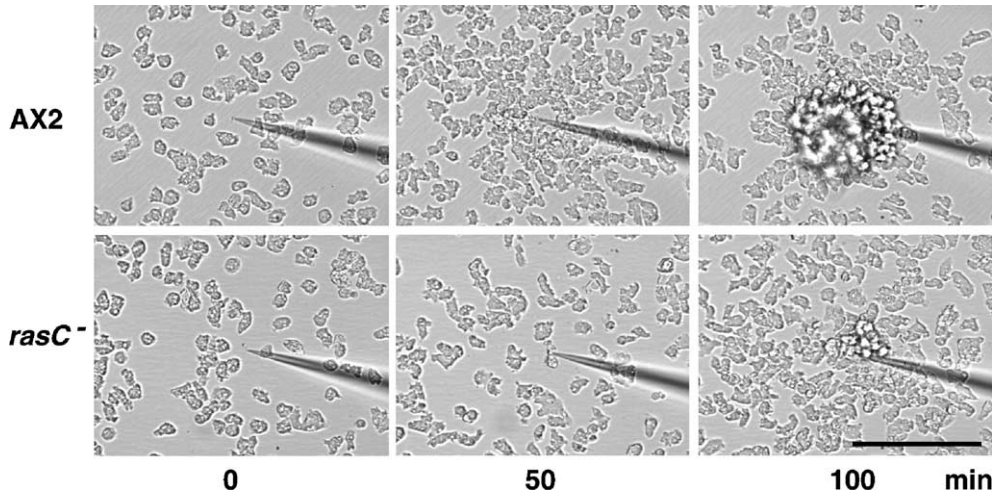

Fig. 1. Chemotaxis in a spatial folate chemoattractant gradient. AX2 and *rasC*$^{-}$ cells were grown to a density of ~4 × 10^5 cells/cm^2 in Nunc dishes. At t = 0, a micropipette filled with 25 mM folate was inserted into the culture and cell movements were monitored by time-lapse microscopy over 100 min. Images shown are from a single experiment that is representative of at least 3 independent assays. Scale bar: 100 μm.

plastic dishes at low density in HL5 growth media and their movement recorded over a period of 30 min as described in Materials and methods. AX2 cells obviously translocated further than the *rasC*$^{-}$ cells (Fig. 2A). However, it was not clear from these data if the *rasC*$^{-}$ cells moved more slowly than the AX2 cells, or whether the two types of cell moved at equal rates and the *rasC*$^{-}$ cells turned more frequently. The movement of the AX2 and *rasC*$^{-}$ cells was therefore scrutinized in more detail. The AX2 cells were observed to be more polar and it was easy to distinguish a front and a back to each cell (Fig. 2B). Furthermore, the pseudopodium at the leading edge was clearly more stable, resulting in cells whose direction of movement was more persistent. In contrast, the *rasC*$^{-}$ cells were more rounded (Fig. 2B) and, although they extended pseudopodia just as frequently as the wild type AX2 cells, these pseudopodia were relatively short-lived and were formed on all sides of the cells. As a result, the cells turned with greater frequency and showed little persistence in direction. Often, an apparent pseudopodium would appear at the uropod, rapidly sending the cell into reverse. Occasionally, a cell produced a pseudopodium that would extend from the upper surface of the cell. Outline plots of two representative cells from each strain over a period of 3.75 min are shown in Fig. 2B and supplemental movies are available at (http://www.sciencedirect.com/science/journal/00144827). These results indicate that loss of RasC reduced the ability of the cell to maintain its leading pseudopod and to continue to move in the same direction. This reduced capability to sustain directional movement could, therefore, explain the reduced chemotaxis to folate shown in Fig. 1.

F-actin distribution

One potential cause for the motility defect in *rasC*$^{-}$ cells might be an aberrant organization of the actin cytoskeleton. In order to address this possibility, vegetative cells were fixed and stained with FITC-phalloidin to visualize F-actin. There were distinct differences in F-actin staining between the AX2 and *rasC*$^{-}$ cells. The characteristic long, thin, actin-rich membrane protrusions termed filopodia [18,19] were much shorter and less frequently observed in *rasC*$^{-}$ cells (Fig. 3). In addition, whereas AX2 cells tended to have a single focus of heavy F-actin staining at the pseudopodial tip or at the leading edge, *rasC*$^{-}$ cells tended to be more rounded and stained heavily for F-actin at several distinct peripheral sites. These patches of F-actin are indicative of multiple pseudopodial extensions and this multiplicity may explain the poor translocation exhibited by *rasC*$^{-}$ cells. It has been suggested that filopodia have the potential to become sites of pseudopodia formation [20,21], and thus, the aberrant regulation of pseudopod formation in *rasC*$^{-}$ cells may be the result of the reduction in number or size of the filopodia.

Transient actin polymerization induced by folate stimulation

The foregoing experiments suggested that the reduced movement of *rasC*$^{-}$ cells in response to folate might simply have been due to a general reduction in motility. In order to determine if the *rasC*$^{-}$ cells exhibited additional defects in folate chemotaxis, we measured the transient polymerization of actin in response to folate stimulation. Suspension grown cells were starved for 30 min in KK2 buffer and stimulated with a single pulse of 50 μM folate. At various time points following stimulation, aliquots of cells were fixed, stained with TRITC-phalloidin and the fluorescence level measured, to assess levels of filamentous F-actin as described in Materials and methods. For AX2 cells, F-actin levels reached a maximum at the earliest measurable time point (5 s) following addition of folate, then rapidly returned to basal levels (Fig. 4A). A similar transient increase in the amount of F-actin was also observed for folate-stimulated

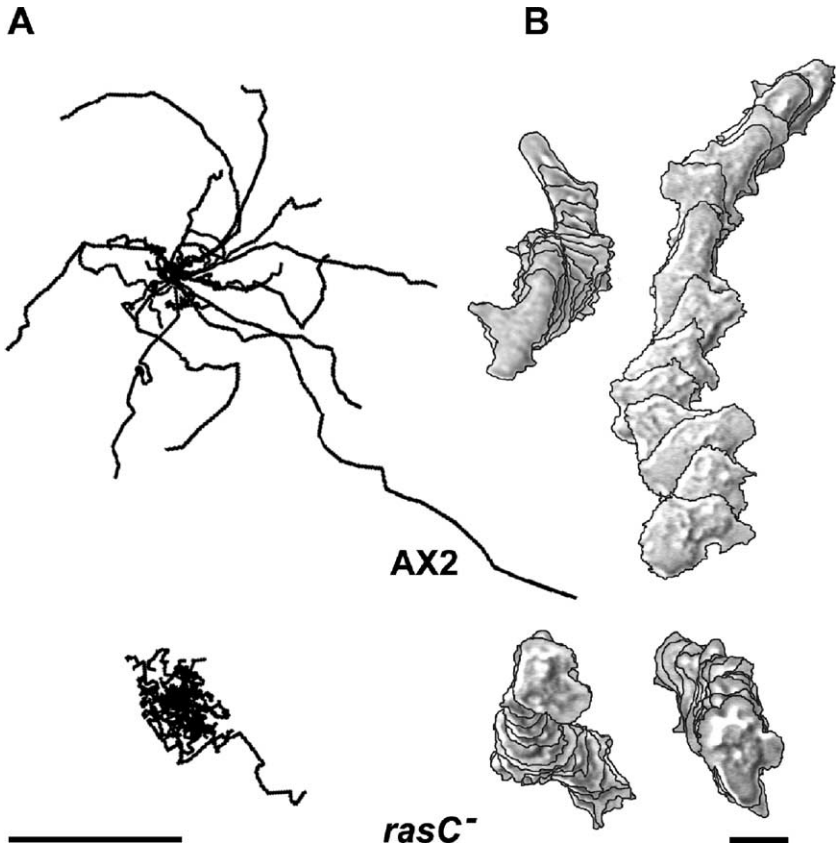

Fig. 2. Random motility of AX2 and *rasC*$^{-}$ cells. (A) Motility tracks of 30 individual AX2 and rasC− amoebae over the course of 30 min were digitally superimposed with the starting points of migration adjusted to the centre of each panel as described under Materials and methods. Scale bar: 100 μm. (B) Cell outline trace of 2 representative AX2 and *rasC*$^{-}$ cells migrating in HL5 growth media. The overlaid images are for 15 frames with a 15-s time interval between each successive frame. Scale bar: 10 μm.

rasC^{-} cells; however, the maximal level at 5 s post-stimulation was considerably lower than that for AX2 cells (Fig. 4A), indicative of a reduced response. Since the distribution of F-actin in unstimulated vegetative *rasC*$^{-}$ and AX2 cells had been found to be different (Fig. 3A), pre-stimulated *rasC*$^{-}$ cells might have had constitutively higher basal levels of F-actin than wild type cells. However, when the total F-actin levels in unstimulated vegetative AX2 and *rasC*$^{-}$ cells were measured, they were found to be not significantly different (Fig. 4B).

Activation of ERK2 and PKB in response to folate

ERK2 is activated in response to stimulation by folate [22] and cells lacking ERK2 exhibit reduced chemotaxis in a folate gradient [23]. To further investigate a possible role for RasC in folate chemotaxis, we measured the phosphorylation of ERK2 in response to folate in *rasC*$^{-}$ cells, using a phospho-MAPK specific antibody that interacts with phosphorylated ERK2, and compared it to the response in AX2. The ~42 kDa protein, that had been shown previously to correspond to ERK2 [12], was rapidly phosphorylated in AX2 and reached a maximum level within 45 s of folate addition. It was then slowly dephosphorylated over the next 2–3 min (Fig. 5A). These kinetics were similar to those previously reported for the response of ERK2 kinase activity to folate [22]. ERK2 was also rapidly phosphorylated in *rasC*$^{-}$ cells, with levels peaking at 45 s following folate stimulation (Fig. 5A), but the level of phosphorylation was lower than that observed for AX2 cells. Thus, although RasC was not essential for the folate-induced phosphorylation of ERK2, loss of RasC modulated the response.

Since PKB is activated and phosphorylated in response to cAMP in aggregating cells and this response is reduced in *rasC*$^{-}$ cells [12,24], we assessed whether PKB might also be phosphorylated in response to folate in vegetative cells. In wild type cells, a ~51 kDa protein, previously identified as PKB [12], was maximally phosphorylated 15 s after the addition of folate, with phosphorylation then returned to a near basal level at 30 s (Fig. 5B). In contrast, this transient increase in PKB phosphorylation was not observed in response to folate in *rasC*$^{-}$ cells (Fig. 5B). These results indicated an involvement of signals normally transduced through RasC for the regulation of PKB in response to folate.

Endocytosis of FITC-dextran

Vegetative *rasS*$^{-}$ cells are highly polarized and exhibit considerably enhanced motility [7], a phenotype opposite of that exhibited by the *rasC*$^{-}$ cells (Fig. 2). Since *rasS*$^{-}$ cells

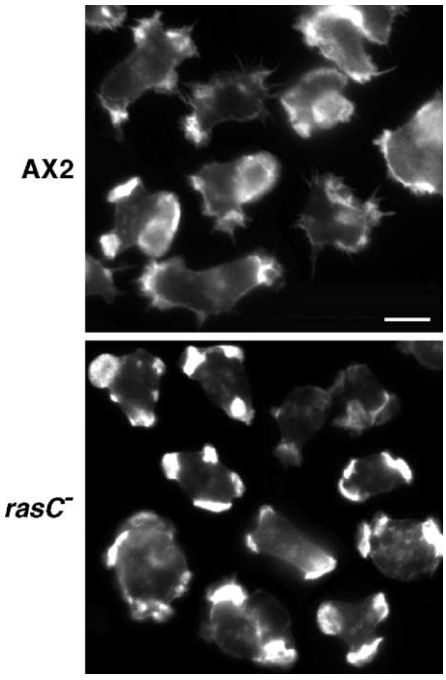

Fig. 3. F-actin distribution in AX2 and *rasC*$^{-}$ cells. Cells were seeded onto glass coverslips in HL5 media and allowed to adhere for 3 h. The media was then removed and the cells immediately fixed with glutaraldehyde, permeabilized with Triton-X100 and stained with TRITC-phalloidin. All cells are shown at the same magnification (100×). Scale bar: 10 μm.

also exhibit lower rates of fluid phase endocytosis, it was suggested [7] that endocytosis and motility might compete for the pool of cytoskeleton constituents, such that the cell is unable to move quickly and undertake endocytosis at high rates at the same time. Since *rasC*$^{-}$ cells move slowly, we examined their ability to endocytose a fluid-phase marker, FITC-dextran. As shown in Fig. 6, *rasC*$^{-}$ cells exhibited greater rates of endocytosis when compared to AX2 cells. In contrast, a RasC overexpression strain (AX2/RasC) exhibited rates of endocytosis that were lower than that of wild type cells, suggesting that RasC protein levels may directly affect this process. The differences in FITC-dextran uptake between the three strains were also apparent when the data were normalized relative to cell protein content rather than to cell number (data not shown).

Regulation of cell size but not cell division

During the course of routinely harvesting *rasC*$^{-}$ cells by centrifugation, it was noticed that the pellet was larger than that for other strains. We therefore performed a quantitative cell-packing assay to determine if this difference was significant. Equal numbers of exponential phase AX2, *rasC*$^{-}$ and AX2/RasC cells were centrifuged in conical volumetric tubes and the pellet volumes were determined. As indicated in the data shown in Table 1, the volume occupied by the *rasC*$^{-}$ cell pellet was significantly greater than that for the AX2 cells. AX2/RasC cell pellet volumes were on average lower, but not significantly different from those of AX2. There was also an increase in the amount of protein per *rasC*$^{-}$ cell compared to the amount for wild type cell (Table 1). Finally, we measured the area occupied by cells that were minimally attached to glass coverslips and found that *rasC*$^{-}$ cells, on average, occupied a larger area than AX2 cells (Table 1). This difference in area does not preclude the possible contribution of a difference in cell spreading between the *rasC*$^{-}$ cells and the wild type cells, but since there was no indication in the appearance of any cell spreading, the measurement probably reflects a genuine

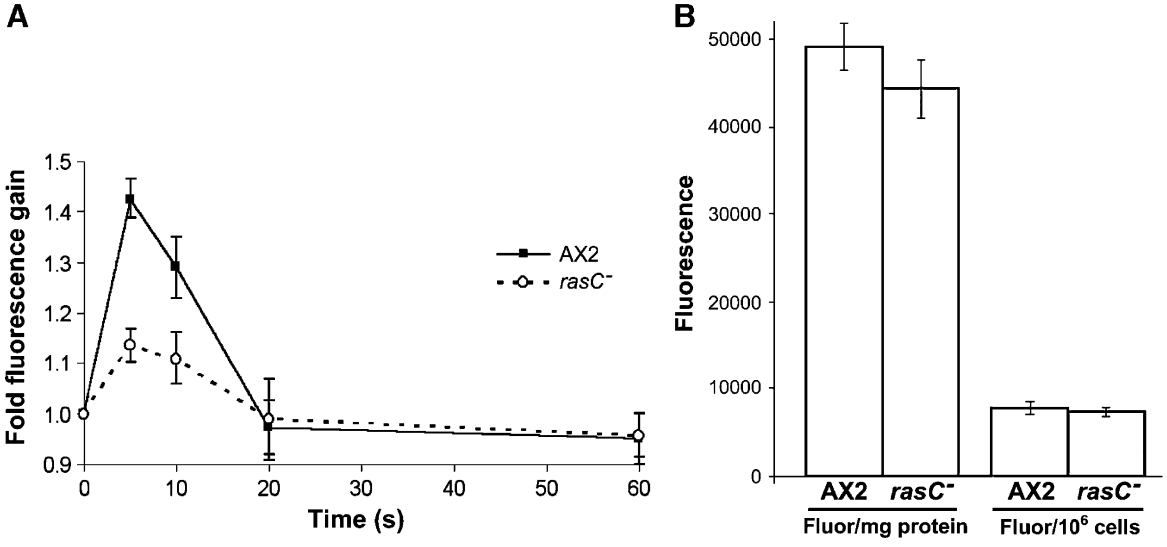

Fig. 4. Basal and folate-stimulated F-actin levels. (A) Folate stimulation of F-actin accumulation. Cells in shaken suspension were stimulated with 50 μM folate and aliquots at the indicated time points were fixed and stained in situ with TRITC-phalloidin and the bound fluorescence determined. The plotted values are normalized relative to the fluorescence at $t = 0$ and are the means ± the standard deviations for 3 independently performed experiments. (B) Basal F-actin levels. Vegetative cells were fixed and stained with TRITC-phalloidin as in (A). The fluorescence values are normalized relative to the protein content or the cell number, as indicated, and are the means ± the standard deviations of 5 replicate determinations.

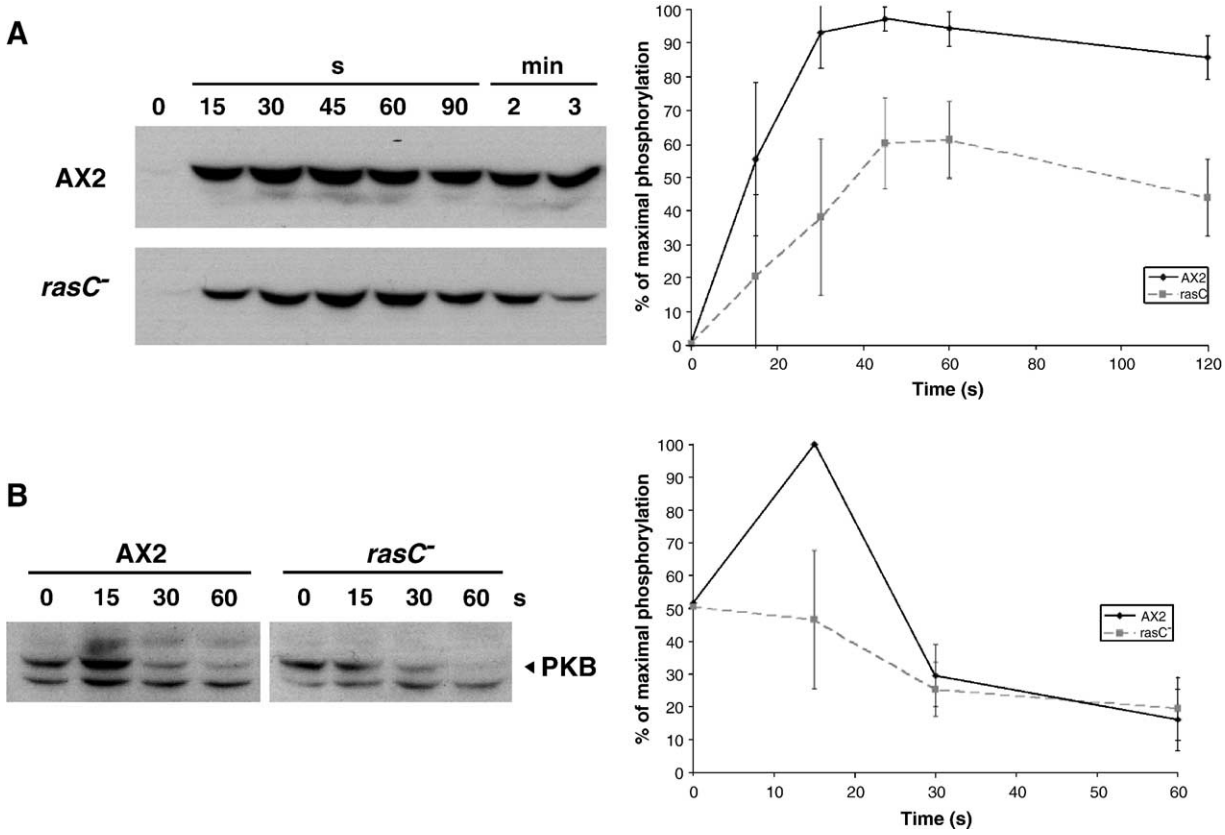

Fig. 5. Folate stimulation of ERK2 and PKB phosphorylation. AX2 and *rasC*$^{-}$ cells in shaken suspension were stimulated with 50 μM folate and cell aliquots, removed at the indicated time points, were lysed directly in SDS-PAGE sample buffer, as described under Materials and methods. 10 μg protein samples were fractionated by SDS-PAGE, blotted and probed with (A) a phospho-MAPK specific antibody or (B) a phospho-threonine specific antibody. Densitometry scans of the results of 3 independently conducted experiments were used to calculate the means ± standard deviation of the folate-induced phosphorylation (shown at right).

difference in cell size. The combined data strongly support the notion that the *rasC*$^{-}$ cells are larger than their wild type counterparts.

Although *rasC*$^{-}$ cells were larger and contained more protein than AX2 cells, the doubling rate in suspension culture of the two strains was similar and the cultures reached comparable terminal cell densities (Fig. 7). AX2 and *rasC*$^{-}$ cells also had a similar nuclear number; average values of 1.5 ± 0.1 and 1.6 ± 0.1 nuclei per cell, respectively, were obtained from a total of 400 cells scored. These results indicate that, although the loss of RasC function was associated with increased cell size, it had no appreciable effect on cytokinesis or nuclear division.

Discussion

We previously reported that *rasC*$^{-}$ cells are unable to progress through aggregative development [12]. It is clear from the results described here that vegetative *rasC*$^{-}$ cells also differed in a number of properties from the parental AX2 cells. They exhibited reduced motility, reduced polarity, enhanced endocytosis and increased cell size, all of which might be related to an altered regulation of the actin cytoskeleton. Consistent with this supposition, filamentous actin was differently distributed in *rasC*$^{-}$ cells compared to wild type cells and F-actin polymerization in response to folate was reduced. These results suggested that signal transduction through RasC plays a role in the coordinated regulation of the cytoskeletal network in the vegetative cell.

Loss of RasC resulted in several changes in vegetative cell motility. When observed in rich axenic media, vegetative AX2 cells remained reasonably polar and persisted in their direction of movement for prolonged periods, often as long as 30 min. In contrast, vegetative *rasC*$^{-}$ cells were more rounded and exhibited a more random motility. The persistent directional movement of AX2 cells was somewhat surprising considering the fact that they were uniformly bathed in nutrient; nevertheless, this behavior has been reported by others [25]. It has been shown elsewhere that when *rasC*$^{-}$ cells were pulsed with cAMP for several hours and observed in the absence of chemoattractant, they displayed problems in maintaining a single anterior pseudopodium [13]. There were more side projections in perimeter tracks and a greater instability of the anterior ends, which at times bifurcated and at other times extended vertically off the substratum. Thus, there were abnormalities in the regulation of anterior pseudopod

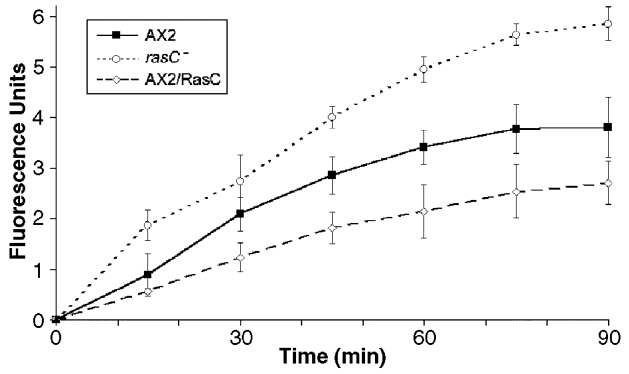

Fig. 6. Fluid phase endocytosis. Uptake of FITC-dextran was determined at the indicated times as described under Materials and methods. The plotted values are arbitrary fluorescence units per 4×10^6 cells, obtained by subtraction of the value at t = 0, and are the means ± the standard deviation of 3 independent experiments.

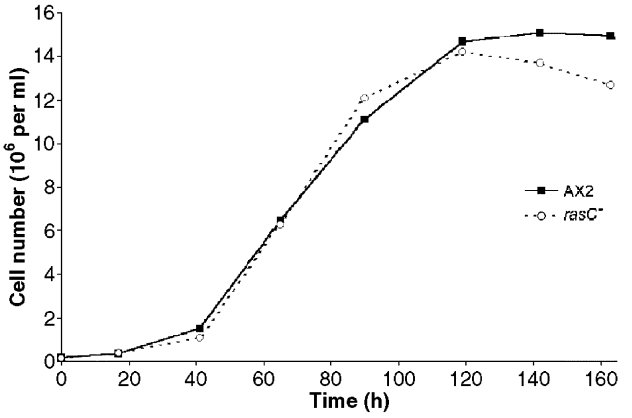

Fig. 7. Growth in suspension culture. AX2 and *rasC*$^-$ cell numbers were determined at the indicated times by hemocytometer counts. The data are for a single experiment, but similar data were obtained for three independent experiments.

formation and maintenance that were shared between the vegetative and starving, cAMP-pulsed *rasC*$^-$ cells. It is not possible to tell given our current understanding how signals that depend on RasC interact with the cellular network that controls movement. Since the *rasC*$^-$ strain is a loss of function mutation, these results suggest that signal transduction through RasC suppresses the propensity for extension of filopodia and thus pseudopodia formation orthogonal to the direction of movement.

We have previously shown that PKB phosphorylation, in response to cAMP, is reduced in developing *rasC*$^-$ cells [12], and in this report, we showed that the response to folate is also reduced in vegetative *rasC*$^-$ cells. PKB phosphorylation has been linked to the generation of cellular asymmetry needed for directed movement during chemotaxis. Potentially, the *rasC*$^-$ vegetative cell phenotypes resulted from altered signaling through PKB, although an independent parallel pathway is also possible. The observation that *rasC*$^-$ cells can form aggregates after cAMP pulsing indicates that after development commences, there must be signal transduction pathways that override the RasC dependant pathway such that loss of the RasC derived signal is less significant.

A number of gene deletion strains exhibit a decrease in fluid phase endocytosis [26] but the enhanced endocytosis of the *rasC*$^-$ cells is, to our knowledge, the first such phenotype to be reported for a *Dictyostelium* gene deletion strain. *rasS*$^-$ cells have an opposite phenotype to *rasC*$^-$ cells in that they exhibit reduced endocytosis and enhanced motility. The *rasS*$^-$ vegetative cell phenotype has been interpreted as a possible competition between endocytosis and motility for the same limited pool of cytoskeletal components [7]. It is unlikely that the enhanced endocytosis and reduced motility exhibited by *rasC*$^-$ cells was due to a similar competition, since the reduced motility did not seem to be due to a reduction in the ability to form pseudopodia. The staining of F-actin in the *rasC*$^-$ cells and the decrease in filopodial structures suggested that the problem for this mutant was an altered spatial organization of actin, rather than a lack in the ability to partition actin to the process of movement due to greater consumption by endocytosis of the same pool of actin. Furthermore, if RasC and RasS did compete, then potentially expression of a constitutively activated form of RasC would produce a phenotype similar to that of the *rasS*$^-$ strain, and this is not the case [27]. Overexpression of RacC and Rap1 resulted in decreased rates of fluid-phase endocytosis [28,29], suggesting that these Ras proteins transmit signals that negatively regulate endocytosis. However, the potential relationship between RasC, RacC and Rap1 in fluid-phase endocytosis remains undefined at present.

Table 1
Effect on cell size

	Cell pellet volume (cm^3 per 2.4×10^8 cells)	Protein content (mg per 10^6 cells)	Cell area (μm^2)
AX2	0.136 ± 0.020	0.0983 ± 0.0037	156.3 ± 41.8
rasC$^-$	0.192 ± 0.030	0.1177 ± 0.0044	212.3 ± 93.1
AX2/RasC	0.102 ± 0.017	n/d	n/d

(n/d: not determined).
Values shown are the average and standard deviation of 4 independent experiments for cell pellet, 5 determinations for protein content and 50 cells for cell area.

The increase in nutrient uptake by the *rasC*$^-$ cells was manifested as an increase in protein content and an increase in cell size. The larger *rasC*$^-$ cells exhibited the same generation time as wild type cells and there was no significant increase in nuclear number. Studies with yeast, *Drosophila* and mammalian cells are beginning to define the signaling components governing cell size regulation [30,31]. Common signaling pathways are well conserved between *Dictyostelium* and metazoan systems and *Dictyostelium* may prove to be a useful model for studying cell size control. The TOR (target of rapamycin) pathway has recently been implicated in the regulation of nutrient sensing, uptake and cell size [30,31]. A relatively newly discovered member of the Ras subfamily of GTPases, Rheb, has been shown to act upstream of TOR in the regulation of

cell size in *Drosophila* [32]. *Dictyostelium* Rheb and TOR orthologs have been predicted from the available genome sequence and we have begun the characterization of the corresponding gene deletion strains, since it is possible that such a pathway involves signals transmitted by a pathway that includes RasC as a component.

The nature of the vegetative cell signaling pathways regulated by RasC are at this stage unknown. Since signaling through RasC appears to be a negative regulator of endocytosis, it could be part of a pathway that monitors the nutrient status of the cell. Thus, if nutrients are plentiful, their uptake would be controlled. RasC also appears to be part of a signaling pathway that is a positive regulator of directional movement that could again be monitoring nutrient status, potentially signaling for increased movement when nutrient is depleted.

Appendix A. Supplementary data

Supplementary data associated with this article can be found, in the online version, at doi:10.1016/j.yexcr.2005.02.002.

References

[1] H.R. Bourne, D.A. Sanders, F. McCormick, The GTPase superfamily: conserved structure and molecular mechanism, Nature 349 (1991) 117–127.

[2] S.L. Campbell, R. Khosravi-Far, K.L. Rossman, G.J. Clark, C.J. Der, Increasing complexity of Ras signaling, Oncogene 17 (1998) 1395–1413.

[3] G.W. Reuther, C.J. Der, The Ras branch of GTPases: Ras family members don't fall far from the tree, Curr. Opin. Cell Biol. 12 (2000) 157–165.

[4] A. Wilkins, R.H. Insall, Small GTPases in *Dictyostelium*: lessons from a social amoeba, Trends Genet. 17 (2001) 41–48.

[5] J. Daniel, G.B. Spiegelman, G. Weeks, *Dictyostelium* ras genes, in: M. Zerial, L.A. Huber (Eds.), Guidebook to the Small GTPases, Oxford University Press, NY, 1995.

[6] C.D. Reymond, R.H. Gomer, M.C. Mehdy, R.A. Firtel, Developmental regulation of a *Dictyostelium* gene encoding a protein homologous to mammalian Ras protein, Cell 39 (1984) 141–148.

[7] J.R. Chubb, A. Wilkins, G.M. Thomas, R.H. Insall, The *Dictyostelium* RasS protein is required for macropinocytosis, phagocytosis and the control of cell movement, J. Cell Sci. 113 (2000) 709–719.

[8] A. Wilkins, M. Khosla, D.J. Fraser, G.B. Spiegelman, P.R. Fisher, G. Weeks, R.H. Insall, *Dictyostelium* RasD is required for normal phototaxis, but not differentiation, Genes Dev. 14 (2000) 1407–1413.

[9] R.I. Tuxworth, J.L. Cheetham, L.M. Machesky, G.B. Spiegelman, G. Weeks, R.H. Insall, *Dictyostelium* RasG is required for normal motility and cytokinesis, but not growth, J. Cell Biol. 138 (1997) 605–614.

[10] B.W. Sutherland, G.B. Spiegelman, G. Weeks, A Ras subfamily GTPase shows cell cycle-dependent nuclear localization, EMBO Rep. 2 (2001) 1024–1028.

[11] R. Kang, H. Kae, H. Ip, G.B. Spiegelman, G. Weeks, Evidence for a role for the *Dictyostelium* Rap1 in cell viability and the response to osmotic stress, J. Cell Sci. 115 (2002) 3675–3682.

[12] C.J. Lim, G.B. Spiegelman, G. Weeks, RasC is required for optimal activation of adenylyl cyclase and Akt/PKB during aggregation, EMBO J. 20 (2001) 4490–4499.

[13] D. Wessels, R. Brincks, S. Kuhl, V. Stepanovic, K.J. Daniels, G. Weeks, C.J. Lim, G. Spiegelman, D. Fuller, N. Iranfar, W.F. Loomis, D.R. Soll, RasC plays a role in transduction of temporal gradient information in the cyclic-AMP wave of *Dictyostelium* discoideum, Eukaryotic Cell 3 (2004) 646–662.

[14] D.J. Watts, J.M. Ashworth, Growth of myxamoebae of the cellular slime mould *Dictyostelium* discoideum in axenic culture, Biochem. J. 119 (1970) 171–174.

[15] S.J. Palmieri, T. Nebl, R.K. Pope, D.J. Seastone, E. Lee, E.H. Hinchcliffe, G. Sluder, D. Knecht, J. Cardelli, E.J. Luna, Mutant Rac1B expression in *Dictyostelium*: effects on morphology, growth, endocytosis, development, and the actin cytoskeleton, Cell Motil. Cytoskeleton 46 (2000) 285–304.

[16] J. Sambrook, E.F. Fritsch, T. Maniatis, Molecular cloning. A laboratory manual, second ed., Cold Spring Harbor Laboratory Press, Cold Spring Harbor, 1989.

[17] J.H. Blusch, W. Nellen, Folate responsiveness during growth and development of *Dictyostelium*—separate but related pathways control chemotaxis and gene regulation, Mol. Microbiol. 11 (1994) 331–335.

[18] Y.H. Han, C.Y. Chung, D. Wessels, S. Stephens, M.A. Titus, D.R. Soll, R.A. Firtel, Requirement of a vasodilator-stimulated phosphoprotein family member for cell adhesion, the formation of filopodia, and chemotaxis in *Dictyostelium*, J. Biol. Chem. 277 (2002) 49877–49887.

[19] J.L. Rifkin, R.A. Speisman, Filamentous extensions of vegetative amoebae of the cellular slime mold *Dictyostelium*, Trans. Am. Microsc. Soc. 95 (1976) 165–173.

[20] J.V. Small, T. Stradal, E. Vignal, K. Rottner, The lamellipodium: where motility begins, Trends Cell Biol. 12 (2002) 112–120.

[21] A.J. Koleske, Do filopodia enable the growth cone to find its way? Sci. Signal Transduct. Knowl. Environ. (2003) e20.

[22] M. Maeda, R.A. Firtel, Activation of the mitogen-activated protein kinase ERK2 by the chemoattractant folic acid in *Dictyostelium*, J. Biol. Chem. 272 (1997) 23690–23695.

[23] Y. Wang, J. Liu, J.E. Segall, MAP kinase function in amoeboid chemotaxis, J. Cell Sci. 111 (1998) 373–383.

[24] R. Meili, C. Ellsworth, S. Lee, T.B.K. Reddy, H. Ma, R.A. Firtel, Chemoattractant-mediated transient activation and membrane localization of Akt/PKB is required for efficient chemotaxis to cAMP in *Dictyostelium*, EMBO J. 18 (1999) 2092–2105.

[25] M. Dumontier, P. Hocht, U. Mintert, J. Faix, Rac1 GTPases control filopodia formation, cell motility, endocytosis, cytokinesis and development in *Dictyostelium*, J. Cell Sci. 113 (2000) 2253–2265.

[26] J. Cardelli, Phagocytosis and macropinocytosis in *Dictyostelium*: phosphoinositide-based processes, biochemically distinct, Traffic 2 (2001) 311–320.

[27] C.J. Lim, G.B. Spiegelman, G. Weeks, Cytoskeletal regulation by *Dictyostelium* Ras subfamily proteins, J. Muscle Res. Cell Motil. 23 (2002) 729–736.

[28] D.J. Seastone, E. Lee, J. Bush, D. Knecht, J. Cardelli, Overexpression of a novel rho family GTPase, RacC, induces unusual actin-based structures and positively affects phagocytosis in *Dictyostelium* discoideum., Mol. Biol. Cell 9 (1998) 2891–2904.

[29] D.J. Seastone, L.Y. Zhang, G. Buczynski, P. Rebstein, G. Weeks, G. Spiegelman, J. Cardelli, The small Mr Ras-like GTPase Rap1 and the phospholipase C pathway act to regulate phagocytosis in *Dictyostelium* discoideum, Mol. Biol. Cell 10 (1999) 393–406.

[30] B.D. Manning, L.C. Cantley, Rheb fills a GAP between TSC and TOR, Trends Biochem. Sci. 28 (2003) 573–576.

[31] L.J. Saucedo, B.A. Edgar, Why size matters: altering cell size, Curr. Opin. Genet. Dev. 12 (2002) 565–571.

[32] P.H. Patel, N. Thapar, L. Guo, M. Martinez, J. Maris, C. Gau, J.A. Lengyel, F. Tamanoi, *Drosophila* Rheb GTPase is required for cell cycle progression and cell growth, J. Cell Sci. 116 (2003) 3601–3610.